Electrical and Thermal Properties of γ-Irradiated Nitrile Rubber/Rice Husk Ash Composites

Rasha M. Mohamed, Reda M. Radwan, Mohamed M. Abdel-Aziz, Magdy M. Khattab

National Center for Radiation Research and Technology, Atomic Energy Authority,
P.O. Box 29, Nasr City, Cairo, Egypt

ABSTRACT: The effects of both the rice husk ash (RHA) loading and fumed silica (FS) loading on the structure, thermal stability, and electrical properties of acrylonitrile–butadiene rubber (NBR) composites were studied. The filler loading were chosen to be 5 and 20 phr for RHA and 5 and 30 phr for silica. Also, the effect of the γ-irradiation dose (25 kGy) on these parameters was investigated. The structure and thermal stability were studied with X-ray diffraction and thermogravimetric analysis techniques. Furthermore, some electrical parameters, such as the direct-current electrical conductivity (σ_{dc}), activation energy (E_a), dielectric constant (ε'), and dielectric loss (ε''), were determined. The incorporation of both RHA and FS resulted in improved thermal stability after γ irradiation at 25 kGy. The loading of FS on NBR was shown to decrease σ_{dc}, ε', and ε'' and increase E_a. On the other hand, the loading of RHA showed the opposite trend. Finally, γ irradiation of NBR composites filled with both fillers decreased the values of σ_{dc}, ε', and ε'' for all the samples, which followed the trend for the unirradiated composites. © 2009 Wiley Periodicals, Inc. J Appl Polym Sci 115: 1495–1502, 2010

Key words: dielectric properties; radiation; rubber; silicas; thermal properties

INTRODUCTION

Silica has been used as a reinforcing filler in the rubber industry for decades.[1] Generally, silica is classified as a highly reactive and polar filler because it contains a large number of silanol groups (Si—OH) on the surface. Such groups have a strong influence on the surface energy of silica. The presence of silanol groups on the silica surface induces strong particle–particle interactions, giving rise to a high tendency for filler agglomeration in the rubber matrix.[2] For this reason, silica is more difficult to disperse and to process in comparison with other fillers. Therefore, a silane coupling agent, a bifunctional compound, is widely used to improve the reinforcing efficiency of silica by enhancing the rubber–filler interaction via chemical linkages.[3–6] The use of silica has recently become more important in the rubber industry, particularly in tire applications, because it provides several advantages over carbon black; that is, silica in tire treads improves the rolling resistance, wear resistance, and wet fraction, provided that it is used in combination with a silane coupling agent.[4,7]

Rice husk ash (RHA), which is an agricultural waste and a fibrous material, can be a source of many silicon-based materials if burned under controlled conditions; several types of RHA can be yielded, depending on the silica content and the carbon black and mineral oxide residuals. The produced silica is slightly colored, semicrystalline, and ultrafine in size and has a large and reactive surface area. Therefore, silica from RHA as a filler material in the rubber industry has been used during the last decade,[8–12] and this makes RHA an ideal starting material as a silica source for preparing advanced materials. However, the results are inferior to those of commercial precipitated silica reported by Fetterman.[13] A general conclusion from these results is the importance of attempting to enhance filler–matrix compatibility through changes in the matrix type and/or the employment of coupling agents.[14] Furthermore, there are other issues with silica ash that need to be resolved, and other approaches are needed to enhance the filler–matrix interaction.

Acrylonitrile–butadiene rubber (NBR) has great potential in industry because of its moderate cost, excellent resistance to oils, fuels, and greases, and easy processability. About 80% of the NBR that is produced is used for machinery and the automobile industry.[15] High-energy ionizing radiation has recently received a great deal of attention for many reasons, including its ability to crosslink various polymers, the lower cost of processing, and the inherently waste-free nature of the technology. It is well

known that the exposure of crosslinking-type polymers to radiation provides improved stability and mechanical properties.[16,17] NBR is a crosslinking-type rubber when it is exposed to high-energy radiation. Compared with the conventional chemical processes used for the crosslinking of rubber, radiation crosslinking has some advantages: it is faster and more versatile, leads to uniform crosslinking, and consumes less energy, and the technology is by its nature inherently waste-free. In addition, considerable efforts have been made to use silicon-rich RHA as a source of semiconductor-grade silicon.[18–20] The study of the electrical properties of NBR is of great importance because of its large utilization in electrical and electronic applications. Generally, conductive and semiconductive rubbers are used for electrostatic charge dissipation, touch control switches, pressure sensors, and so forth.[21,22] The electrical conductivity of these rubbers depends on various factors, such as the type of polymer matrix, the conductive or semiconductive filler, and the filler loading.[23] Also, γ irradiation of NBR composites may induce some changes in their electrical behaviors.[24,25] Ishak and Bakar[10] reported that better mechanical properties of silica-ash-filled vulcanizates were achieved with approximately 20 wt % silica ash. Increasing the filler loading showed that the silica ash composites suffered from lower filler–matrix interactions; this was evident from the poorer tensile properties and reduced elongation at break (%) at higher filler loadings. The blending conditions and the optimum concentration of the RHA and silica loading for obtaining the best mechanical properties have been reported.[26] Therefore, in this study, two concentrations of RHA (5 and 20 phr) were chosen. In addition and for comparison, two concentrations of fumed silica (FS; 5 and 30 phr) were selected. Because NBR enhanced with trimethylol propane trimethacrylate (TMPTMA) is crosslinked by γ-irradiation doses ranging from 20 to 30 kGy,[27,28] the influence of the γ-irradiation dose, namely 25 kGy, on the these properties was studied.

In this study, a grade of RHA with a high content of silica (87.79%), in addition to carbon black and metal oxide residues, was selected as a low-cost filler for NBR rubber to study its performance. A widely used commercial grade of FS was also used to compare its performance with that of RHA. The thermal stability of the NBR composite and the composites filled with both RHA and FS was studied with the thermogravimetric analysis (TGA) technique. Besides, X-ray diffraction (XRD) was used to follow the semicrystalline phase of RHA. Also, this work was extended to study the electrical properties of NBR composites through the determination of the direct-current electrical conductivity (σ_{dc}) and activation energy (E_a) as well as the dielectric constant

TABLE I
Chemical Composition of RHA

Chemical substance	Amount (wt %)
SiO_2	87.79
CaO	1.24
Al_2O_3	0.4
Fe_2O_3	0.37
MgO	1.59
P_2O_5	4.74
K_2O	1.69
Loss of ignition	2.08

(ε') and dielectric loss (ε'') because composites loaded with silica are recommended for use in insulation applications. Finally, the influence of a 25-kGy γ-irradiation dose on the above mentioned parameters was investigated.

EXPERIMENTAL

Materials

The materials used were NBR (Krynac 3950) with a high acrylonitrile content (39.5 wt %) and FS (asil grade) and semicrystalline RHA as fillers. RHA was obtained via the burning of rice husks in a muffle furnace at 700°C for 2 h. It had a very low bulk density (ca. 0.13 g/cm^3). The other chemicals, such as zinc oxide and stearic acid, were commercial-grade materials. TMPTMA was obtained from Aldrich Chemical Co., Ltd. A coupling agent, 3-aminopropyl triethoxysilane (3-APE), was supplied by Fluka. The chemical compositions and physical properties of RHA and FS are presented in Tables I and II.

Filler treatment

The coupling agent, 3-APE, was provided in a liquid form; it was diluted in ethanol to make a 20% solution. The concentrations of 3-APE were 1 and 8 wt % for RHA and FS, respectively. The proposed amounts were previously found to be appropriate for obtaining the optimum properties of vulcanizates.[12,29,30]

Compounding and processing

The compounding of the rubber was carried out on a laboratory-scale two-roll mill. The rubber was first masticated for 5 min, and the additives were added sequentially, as shown in Table III. Then, the compounding was continued for 30 min to ensure homogeneous mixing of the additives. Sheets 1 mm thick were prepared with a hot press at 100°C for 5 min, and this was followed by cold pressing for 2 min. The composite specimens are labeled as illustrated in Table III.

TABLE II
Physical Properties of FS and RHA

Parameter	FS	RHA
Surface area (m^2/g)	170–230	45
Density (g/cm^3)	2.2	0.13

Irradiation process

The NBR composites were irradiated with γ radiation up to 25 kGy from a ^{60}Co source at a dose rate of 6.25 kGy/h.

TGA

TGA of a polymeric material gives an idea about its composition and thermal stability. Furthermore, a detailed understanding of the degradation of polymers due to heating is relevant for designing materials with improved properties for specific applications. The TGA studies were carried out with a Shimadzu (Japan) TGA-30 apparatus at a heating rate of 10°C/min in nitrogen from room temperature up to 600°C.

Structural properties (XRD)

XRD analysis was used to study the changes in the crystalline phases of the proposed samples because RHA or silica ash, as it is commonly called, is classified as industrial waste and, depending on the combustion conditions, contains approximately 55–97% silica in partially crystalline and amorphous forms, the rest being an amalgamation of carbon impurities and a small fraction of metal oxide impurities. The structural properties of the filler before and after treatment with the silane coupling agent and the composites filled with both fillers were investigated with an XRD instrument. The XRD instrument was a Shimadzu model XD-D1 with a wavelength of 0.15425 nm for Cu Kα1. The XRD pattern was performed in the 2θ angle of 4–30°.

Electrical properties

The electrical properties of the composites were influenced by the intrinsic electrical properties of the constituents, temperature, frequency, and mechanical stress. Furthermore, microstructural effects (e.g., the filler concentration, filler shape, filler size, and spatial distribution of the filler particles) also played an important role in the composite properties. For electrical measurements, an air-drying silver paste was applied to the opposite surfaces of NBR samples in a sandwich configuration to ensure good electrical contacts. For the direct-current (dc) measurements, a Keithley type 6517A digital electrometer (USA) was used for the determination of the dc resistance of the samples. The samples were mounted

in an oven, in which the temperature of the samples was monitored with a K-type thermocouple attached to a Tri-Sense digital thermometer (Cole-Parmer) with a temperature resolution of 0.1°C. The value of the applied voltage was selected after I–V characteristic testing was performed for all samples, providing linear ohmic behavior in the range of 0–100 V. The sample temperature was varied from 293 to 373 K during the measurements. The alternating-current measurements were carried out with a Hioki (Japan) 3531 Z Hi-Tester LCR meter operating at a frequency range of 42 Hz to 5 MHz with an impedance accuracy ranging from 0.15 to 4%. The dielectric measurements were performed at room temperature in a frequency range of 100 Hz to 5 MHz. The LCR meter was connected to the computer through an RS-232C interface.

RESULTS AND DISCUSSION

Thermal decomposition behavior

Thermograms of the NBR blank and the composites containing both RHA and FS before and after γ exposure up to 25 kGy are presented in Figures 1 and 2 and Table IV. For the unirradiated blank NBR sample, there was almost no weight loss up to 394°C. For higher temperature levels, two stages of degradation were noticed. The first stage started at 414°C with a weight loss of 7.3% and completed at 473.3°C; it resulted in a weight loss of 58.6%. In the second stage, the degradation started at 493.98°C with a weight loss of 65.8% and ended with a weight loss of 91.8% at 600°C. The two decomposition stages corresponded to degradation by random chain scission of the butadiene and acrylonitrile parts in NBR. The obtained results were shown to be in close agreement with those results obtained by George et al.[31] The first stage, which started at 414°C, led to a weight loss of 80.37% and completed at 526.76°C. In the second stage, the degradation started at 543.6°C and completed at 633°C with a weight loss of 11.86%.

In the case of the composites filled with 5 or 30 phr FS, the addition of FS resulted in a shift in the

TABLE III
Formulation Composition

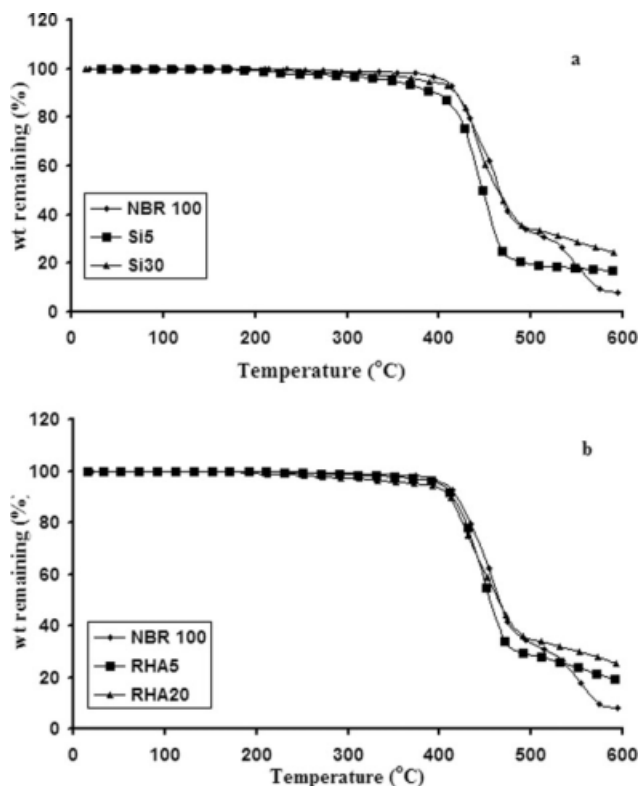|	Recipe content (phr)				
Sample	NBR	ZnO	Stearic acid	Treated RHA and FS	TMPTMA
NBR$_{100}$	100	5	1	0	2
RHA$_5$	100	5	1	5 (RHA)	2
RHA$_{20}$	100	5	1	20 (RHA)	2
Si$_5$	100	5	1	5 (silica)	2
Si$_{30}$	100	5	1	30 (silica)	2

Figure 1 TGA thermograms for unirradiated NBR composites with and without (a) FS and (b) RHA.

initial decomposition temperature. Table IV illustrates the temperature at which 10% degradation occurred ($T_{0.1}$) as a measure of the onset of the degradation and the temperature at which 50% degradation occurred ($T_{0.5}$) as the midpoint of the degradation process. These values were lower than those for the NBR composite. Also, the weight-loss rate of the two NBR composites filled with FS eventually slowed versus that of the NBR composite at an elevated temperature. The two concentrations of FS residues were 83.4 and 76.9 wt %, respectively, at about 580°C. With increasing temperature, the weight-loss rate became slower. It is interesting that the thermal decomposition of the NBR composites filled with the two concentrations of FS had similar degradation processes. From this, it could be concluded that the composite filled with FS was less stable than the NBR composite. The obtained results can be explained by the interaction between nitrile groups and silica, as reported by Choi[32] and Suzuki et al.[33] They suggested that the dispersity of silica particles is improved by nitrile groups as the agglomeration of silica is due to hydrogen bonding between silanol groups on the silica surface with nitrile groups. Hence, the agglomeration is suppressed by hydrogen bonding with the nitrile groups, and this results in the disappearance of the degradation peak of acrylonitrile parts in NBR. The same trend was obtained for the composites filled with 5 or 20 phr
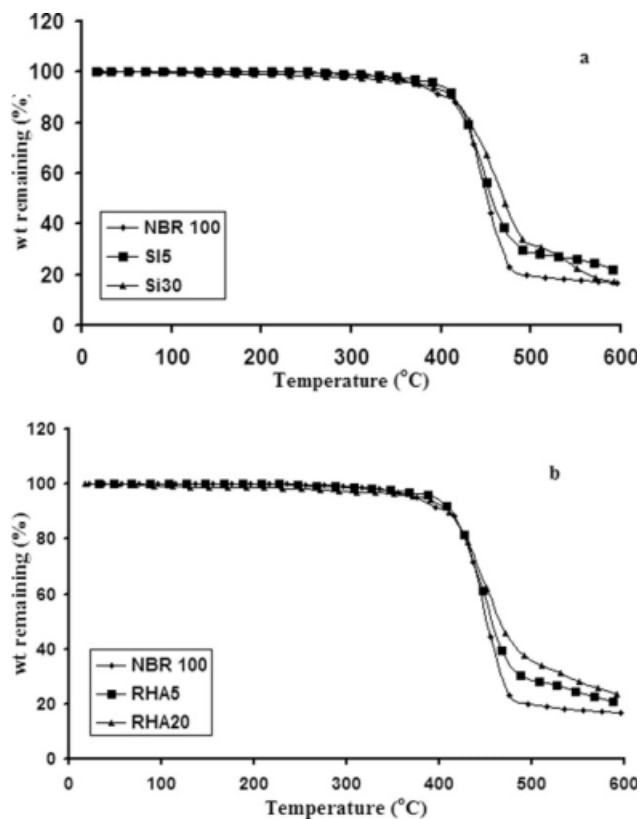
Figure 2 TGA thermograms for NBR composites with and without (a) FS and (b) RHA exposed to 25 kGy of γ irradiation.

RHA; that is, the initial decomposition temperature was shifted to 391.7°C, and the degradation was in one step.

Thermograms of the γ-irradiated NBR composite filled with both RHA and FS are shown in Figure 2. In the case of the irradiated NBR composite, the irradiation of the NBR sample led to reduced thermal stability; that is, the temperature at which the initial weight loss occurred decreased to 376.9°C in comparison with the temperature of the unirradiated one (394°C). Moreover, the degradation of the irradiated NBR sample occurred in one stage. This can be attributed to the addition of a polyfunctional

TABLE IV
TGA Results for the NBR, NBR-Filled FS, and RHA Composites

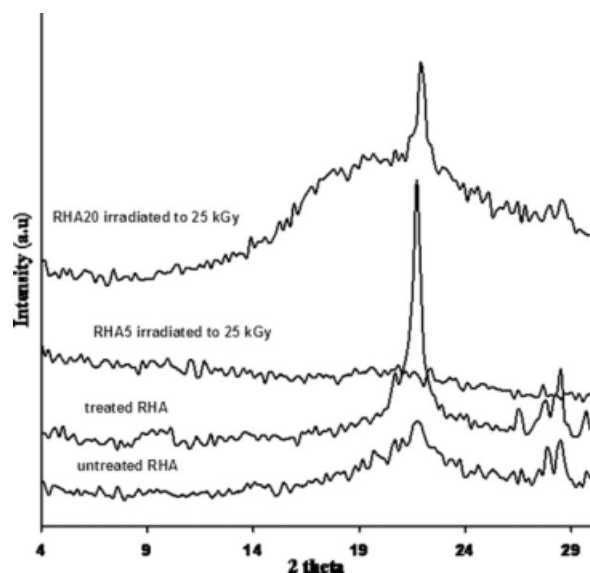|	Sample	$T_{0.1}$ (°C)	$T_{0.5}$ (°C)	Residue (%)
Unirradiated	NBR$_{100}$	423	465	92
	Si$_5$	392	448	83.4
	Si$_{30}$	417	462	76.9
	RHA$_5$	416	454	81.4
	RHA$_{20}$	410	462	75.25
γ-Irradiated	NBR$_{100}$	406	453	80.9
	Si$_5$	416	457	79.28
	Si$_{30}$	413	467	83.4
	RHA$_5$	416	457	80
	RHA$_{20}$	410	467	76.9

Figure 3 XRD patterns of the untreated RHA, treated RHA, and irradiated NBR composites filled with 5- or 20-phr RHA.

monomer (TMPTMA) to NBR, which exerted a detrimental influence on the thermal stability; this could probably be attributed to the formation of low-weight molecules resulting from the radiolysis of TMPTMA. Their interaction in turn with NBR presumably resulted in the retardation of curing.[27] Table IV illustrates $T_{0.1}$, $T_{0.5}$, and the residue at 600°C. We can find out that the onset temperature of the degradation for the two types of composites (FS and RHA) was almost the same for the two ratios and higher than that for the irradiated NBR composite. One might expect the irradiated composites filled with FS and RHA to be thermally stable rather than the irradiated NBR composite. Therefore, the irradiated composite filled with a high concentration of RHA could be classified as thermally stable and could be used in the rubber industry for economical purposes.

XRD analysis

Figure 3 shows the X-ray diffraction patterns for active RHA before and after treatment with the coupling agent as well as the NBR composite filled with both RHA contents and irradiated to 25 kGy. In the XRD patterns of RHA before the silane treatment, two diffraction peaks were observed at 2θ values of 21.75 and 28.55; they represented the diffraction of the crystal surface of layered active RHA corresponding to d-spacings of 4.08 and 3.123 Å, respectively. The obtained results indicated that a relatively large gallery expansion in the layered active RHA was obtained, confirming the semicrystalline phase of RHA. However, for the sample of RHA

treated with the silane coupling agent, the two major peaks appeared at 2θ values of 21.75 and 28.388, with no change in the d-spacing values. In the mean time, their XRD pattern was characterized by an increase in the intensity of the crystalline phase. This was mainly attributed to an irregular arrangement in the structure as a result of the increase in the solid phase, which was composed of atoms arranged in three dimensions, leading to an increase in the crystalline phase. In other words, the reactive silanol groups on the ash surface chemically reacted with the organosilane (silane coupling agent) to form stable siloxane linkages, which were proven effective in enhancing the dispersion, adhesion, and compatibility of silica ash in the polymer matrix.[34]

Also, in the same figure, the XRD pattern for NBR loaded with 5 phr RHA revealed that the addition of 5 phr active RHA treated with the coupling agent to the rubber matrix (NBR) irradiated up to 25 kGy resulted in the disappearance of the diffraction peaks at 2θ values of 21.75 and 28.38. This behavior may be due to the dispersion of the semicrystalline phase of the treated RHA in the NBR matrix. In other words, as mentioned before, there was an interaction between the silica derived from RHA and the nitrile group in NBR. On the other hand, at a higher RHA loading (20 phr), the XRD peaks at 2θ values of 21.75 and 28.38 returned but with less intensity in comparison with the treated RHA. This can be explained by the fact that all the nitrile groups in the acrylonitrile part in the nitrile rubber
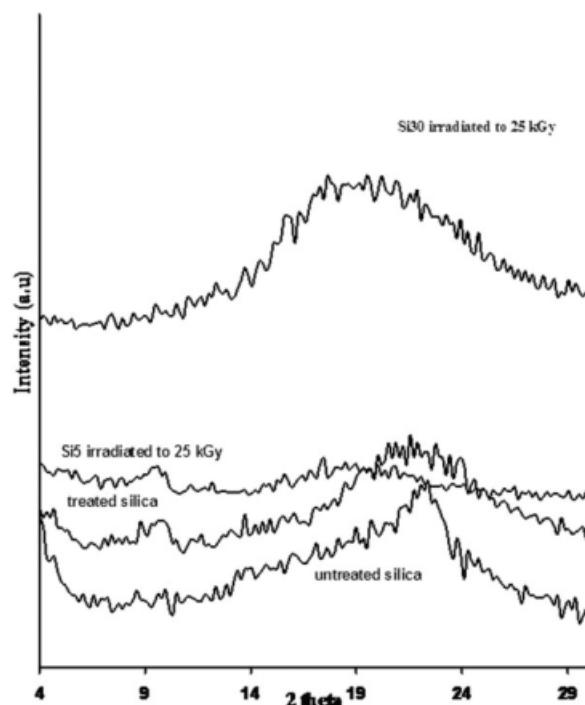

Figure 4 XRD patterns of untreated silica, treated silica, and irradiated NBR composites filled with 5- or 30-phr silica.

TABLE V
Electrical Parameters for the Unirradiated and γ-Irradiated NBR Composites Filled with FS and RHA

	Unirradiated				γ-Irradiated (25 kGy)			
Sample	σ_{dc} (Ω^{-1} m^{-1})	E_a (eV)	R^2 (%)	τ (s)	σ_{dc} (Ω^{-1} m^{-1})	E_a (eV)	R^2 (%)	τ (s)
NBR_{100}	2.56×10^{-8}	0.638	99.83	1.61×10^{-7}	6.9×10^{-9}	0.758	99.04	1.15×10^{-6}
Si_5	8.96×10^{-9}	0.67	99.31	1.52×10^{-7}	6.07×10^{-9}	0.766	98.81	6.71×10^{-7}
Si_{30}	7.56×10^{-10}	0.924	98.48	1.02×10^{-7}	6.93×10^{-10}	0.95	98.86	1.40×10^{-7}
RHA_5	3.75×10^{-8}	0.624	99.4	6.69×10^{-7}	1.01×10^{-8}	0.704	97.78	1.87×10^{-6}
RHA_{20}	6.56×10^{-8}	0.581	99.27	1.60×10^{-6}	1.28×10^{-8}	0.661	99.59	3.35×10^{-6}

interacted with the silica derived from RHA, and there was still excess treated RHA that was unreacted. Therefore, the semicrystalline phase of the treated RHA returned with less intensity.

In contrast, the XRD curves for FS before and after the treatment with the silane coupling agent as well as the NBR composites filled with both FS concentrations and irradiated at 25 kGy are shown in Figure 4. It can be observed from the XRD patterns for FS before and after the silane treatment that there was no change between the untreated and treated FS; that is, the patterns were completely amorphous. In addition, the incorporation of 5 or 30 phr FS into the NBR composites induced no change in the XRD patterns, and the patterns were completely amorphous.

Electrical properties

σ_{dc} was measured for NBR composites at room temperature, and the obtained results are listed in Table V. For the unirradiated blank NBR samples, σ_{dc} was found to be 2.56×10^{-8} Ω^{-1} m^{-1}. With the loading of FS into the NBR samples, σ_{dc} was found to decrease with the concentration of FS increasing. In contrast, the increase in the concentration of the loaded RHA in the NBR samples led to an increase in σ_{dc}. The loading of FS may have led to decreased mobility of the charge carriers due to the linking between the FS molecules and the polymer molecules,[35,36] which, in turn, decreased the electrical conductivity. Meanwhile, this case cannot be applied for the loading of RHA because RHA contains, beside FS, some metal oxides and carbon black, which can increase σ_{dc}.

The γ-irradiation exposure of the samples at 25 kGy was shown to decrease σ_{dc} by the same trend found for the unirradiated composites. The irradiation of NBR may have resulted in crosslinking in all the samples, which decreased the mobility of the free charge carriers in the polymer.[37] Also, it has been suggested that the decrease in σ_{dc} is due to the formation of some defects (traps) in the energy gap as a result of irradiation.[38] These defects create barriers against the mobility of the charge carriers in the polymer.[39]

The study was extended to include the calculation of E_a for all samples. In addition, the conductivity was measured at different temperature levels ranging from 293 to 373 K because the composites were thermally stable in this region. Figure 5 shows the relationship of ln σ_{dc} with $1000/T$, where T is the temperature, for the unirradiated and γ-irradiated NBR samples. For the proposed temperature range, the conductivity was found to increase as a function of temperature for all samples; the plots were found to follow Arrhenius behavior:[39]

$$\sigma_{dc}(T) = \sigma_0 \exp(-E_a/kT) \quad (1)$$

where σ_0 is the temperature-independent constant and k is the Boltzmann constant. The E_a values for the unirradiated and irradiated samples were determined from the slopes of the straight lines obtained from Figure 5. σ_{dc} values and the correlation coefficient for each straight line are listed in Table V. An E_a value of 0.638 eV was reported for the blank NBR sample, whereas it increased with the concentration of FS increasing. On the other hand, E_a was found to
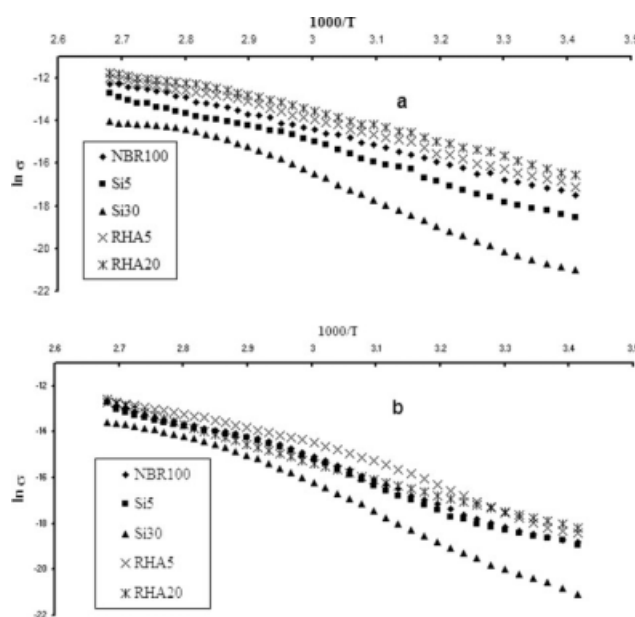
Figure 5 Plots of ln σ_{dc} versus $1000/T$ (K^{-1}) for (a) unirradiated and (b) γ-irradiated NBR loaded with FS and RHA.
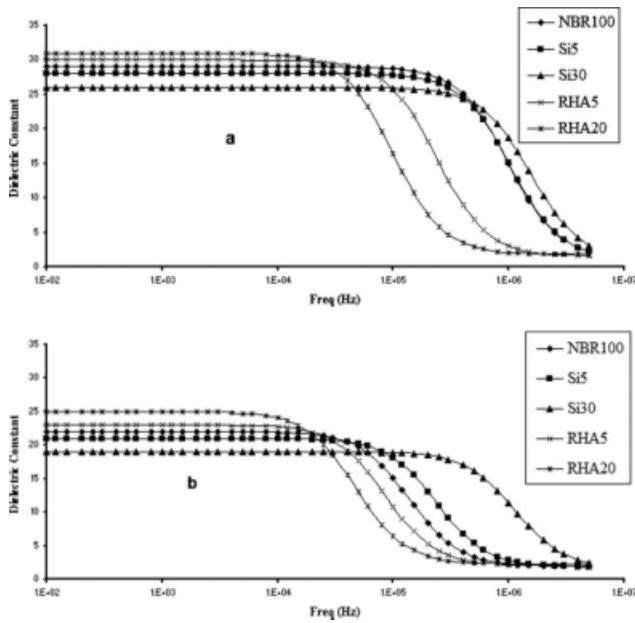
Figure 6 ε' as a function of frequency for (a) unirradiated and (b) γ-irradiated NBR loaded with FS and RHA.

decrease with the RHA concentration increasing in the NBR samples.

Furthermore, the irradiation of NBR led to increased E_a values for all samples, whereas the same behavior was maintained for the unirradiated samples; this supported the results of σ_{dc} at room temperature because the increase in σ_{dc} generally led to a decrease in E_a and vice versa.[40] Moreover, Figure 5 shows that the differences in σ_{dc} became smaller for the irradiated samples. This could be due to the γ-radiation-induced effect on the NBR polymer, which could be the dominant effect on σ_{dc} because the polymer represented the major constituent of these samples.

Measurements of ε' and ε'' of the samples were carried out. The obtained values were used for fitting the following parameters with the Debye equations:[41]

$$\varepsilon' = \varepsilon'_\infty + \frac{\varepsilon'_s - \varepsilon'_\infty}{1 + \omega^2\tau^2} \qquad (2)$$

$$\varepsilon'' = \frac{(\varepsilon'_s - \varepsilon'_\infty)\omega\tau}{1 + \omega^2\tau^2} \qquad (3)$$

where ε'_s is the dielectric constant in a static field, ε'_∞ is the dielectric constant at the end of the frequency range (minimum value of ε'), $\omega = 2\pi f$, ω is the angular frequency, f is the frequency, and τ is the relaxation time. By simple mathematical manipulation, we can get the dielectric parameters in the form of an equation representing a straight line:

$$\varepsilon''/\omega = (\varepsilon' - \varepsilon'_\infty)\tau \qquad (4)$$

or

$$\log(\varepsilon''/\omega) = \log(\varepsilon' - \varepsilon'_\infty) + \log(\tau) \qquad (5)$$

τ for all samples could be determined from the intercept of the straight line in eq. (5); the values are listed in Table V. τ decreased with increasing FS content in the NBR samples, whereas it increased with an increasing RHA concentration in the unirradiated samples. However, the values of τ indicated the existence of dipole relaxation for all the samples.[35,41] Also, γ irradiation was found to induce an increase in the τ value for all samples. Substituting the value of τ into eqs. (2) and (3), we obtained the fitted values of both ε' and ε'' as functions of the frequency, as shown in Figures 6 and 7.

Figure 6(a) shows ε' as a function of the frequency in the range of 100 Hz to 5 MHz for the unirradiated NBR samples. A relaxation decrease in ε' can be clearly seen at about 1 MHz for the unirradiated blank sample. Two opposite shifts in this relaxation can be observed; the first is toward higher frequencies and is due to the loading of FS, whereas the second is toward lower frequencies and is due to the RHA loading. Also, the value of ε' decreased with the concentration of FS increasing; this meant a decrease in the stored charge in NBR. This decrease may be attributed to the linking between FS and NBR, which may have decreased the number of dipoles in the polymer. Meanwhile, the ε' values
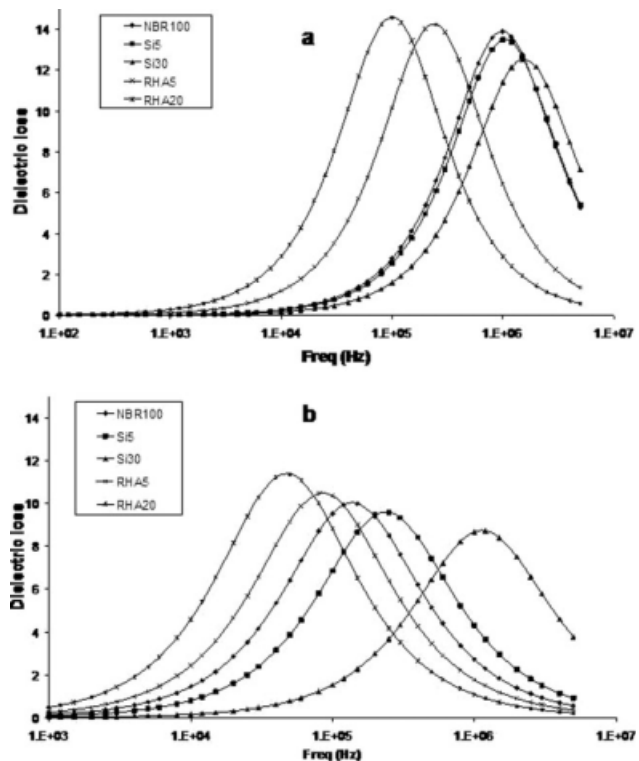

Figure 7 ε'' as a function of frequency for (a) unirradiated and (b) γ-irradiated NBR loaded with FS and RHA.

increased with the concentration of RHA loaded on the polymer increasing because of the increase in the number of dipoles resulting from the metal oxides included in RHA.

However, the irradiation of all NBR samples resulted in a decrease in the ε' values and also shifted the relaxation toward lower frequencies, as shown in Figure 6(b). As discussed previously, the irradiation resulted in crosslinking of the chains of NBR, the major constituent of the composite samples, which may have reduced the ability of the samples to store charge.

The same behavior was clearly seen for ε'' [Fig. 7(a)]; the peak of the maximum loss value slightly increased toward the RHA loading, whereas it slightly decreased toward the FS loading. Also, the peak position obeyed the same trend found for the relaxation of ε'.

By irradiation, the intensity of all peaks was decreased, and their positions were shifted toward lower frequencies. This could be due to the radiation-induced crosslinking, which decreased the inability of dipoles to orient themselves along the field direction in a rapidly varying applied electric field.[35]

CONCLUSIONS

The main objective of this study was to gauge the possibility of using low-cost RHA as an alternative filler matrix in NBR. The irradiated composites filled with 30 phr FS and 20 phr RHA were more thermally stable than the irradiated NBR composite. The dielectric properties were more improved by filling NBR composites with RHA rather than silica.

This study offers a polymeric material with relatively good thermal stability, low electrical conductivity, and high dielectric properties. This suggests the possibility of the utilization of a low-cost RHA-filled NBR composite as a semiconducting polymer. Furthermore, the enhancement of ε' for RHA-filled NBR could enable the composite to be used in thin-layer capacitors.

References

1. Wang, M. J.; Wolff, S. Rubber Chem Technol 1992, 65, 715.
2. Wolff, S.; Wang, M. J. Rubber Chem Technol 1992, 65, 329.
3. Byers, J. T. Rubber World 1998, 218(6), 38.
4. Goerl, U.; Hunsche, A.; Mueller, A.; Koban, H. G. Rubber Chem Technol 1997, 70, 608.
5. Reuvekamp, L. A. E.; Ten Brink, J. W.; Van Swaajj, P. J.; Noordermeer, J. W. M. Rubber Chem Technol 2002, 75, 187.
6. Ten Brinke, J. W.; Debnath, S. C.; Reuvekamp, L. A. E.; Noordermeer, J. W. M. Compos Sci Technol 2003, 63, 1165.
7. Waddell, W. H.; O'Haver, J. H.; Evans, L. R.; Harwell, J. H. J Appl Polym Sci 1995, 55, 1627.
8. Ismail, H.; Mega, L.; Khalil, H. P. S. A. Polym Int 2001, 50, 606.
9. Manna, A. K.; Bhattacharya, A. K.; De, P. P.; Tripathy, D. K.; De, S. K.; Peiffer, D. G. Polymer 1998, 39, 7113.
10. Ishak, Z. A. M.; Bakar, A. A. Eur Polym J 1995, 31, 259.
11. Siriwardena, S.; Ismail, H.; Ishiaku, U. S. Polym Int 2001, 50, 707.
12. Ismail, H.; Nasaruddin, M. N.; Ishiaku, U. S. Polym Test 1999, 18, 287.
13. Fetterman, M. Q. Rubber World 1986, 194, 38.
14. Suzuki, N.; Yatsuyanagi, F.; Ito, M.; Kaidou, H. J Appl Polym Sci 2002, 86, 1622.
15. Brydson, J. A. Rubber Materials and Their Compounds; Elsevier: New York, 1988; p 187.
16. Wilski, H. Radiat Phys Chem 1987, 29, 1.
17. Saunders, C. B. Radiation Processing in the Plastic Industry: Current Commercial Applications; Atomic Energy of Canada Limited Report, AECL-9569; 1988.
18. Govinda Rao, V. M. H. J Sci Ind Res 1980, 39, 495.
19. Amick, J. A. J Electrochem Soc 1982, 129, 864.
20. Hunt, L. P.; Dismukes, J. P.; Amick, J. A.; Schei, A.; Larsen, K. J Electrochem Soc 1984, 131, 1683.
21. Sau, K. P.; Chaki, T. K.; Khastgir, D. J Mater Sci 1997, 32, 5717.
22. Bhadra, S.; Khastgir, D. Eur Polym J 2007, 43, 4332.
23. Pramanik, P. K.; Khastagir, D.; Saha, T. N. J Mater Sci 1993, 28, 3539.
24. Nasr, G. M.; Badawy, M. M.; Ateia, E. Polym Degrad Stab 1993, 60, 333,
25. Abou Zeid, M. M. Eur Polym J 2007, 43, 4415.
26. Mohamed, R. M.; Khattab, M. M.; Abdel-Aziz, M. M. To appear.
27. Yasin, T.; Ahmed, S.; Yoshii, F.; Makuuchi, K. React Funct Polym 2002, 53, 173.
28. Vijayabaskar, V.; Bhowmick, A. K. J Appl Polym Sci 2005, 95, 435.
29. Ismail, H.; Ishiaku, U. S.; Lu, E. S.; Ishak, Z. A. M. Int J Polym Mater 1998, 39, 45.
30. Ismail, H.; Nasaruddin, M. N.; Rozman, H. D. Eur Polym J 1999, 35, 287.
31. George, S.; Varughese, K. T.; Thomas, S. Polymer 2000, 41, 5485.
32. Choi, S. S. J Appl Polym Sci 2002, 85, 385.
33. Suzuki, N.; Ito, M.; Ono, S. J Appl Polym Sci 2005, 95, 74.
34. da Costa, H. M.; Visconte, L. L. Y.; Nunes, R. C. R.; Furtado, C. R. G. J Appl Polym Sci 2003, 87, 1194.
35. Radwan, R. M.; Fawzy, Y. H. A.; El-Hag Ali, A. Radiat Phys Chem 2008, 77, 179.
36. Walszczak, M.; Kroh, J.; Abdel-Hamid, M. M. Radiat Phys Chem 1995, 45, 71.
37. Abdel-Hamid, H. M.; El-Sayed, S. M.; Radwan, R. M. Nucl Instrum Meth B 2004, 215, 479.
38. Hirankumar, G.; Selvasekarapandian, S.; Kuwata, N.; Kawamura, J.; Hattori, T. J Power Sources 2005, 144, 262.
39. Abdel-Hamid, H. M.; Radwan, R. M.; Ashour, A. H. J Phys D: Appl Phys 2002, 35, 1183.
40. Radwan, R. M. Nucl Instrum Meth B 2007, 262, 249.
41. Pethig, R. Dielectric and Electronic Properties of Biological Materials; Wiley: New York, 1979; p 15.